Food Chemistry: X 25 (2025) 102091

Contents lists available at ScienceDirect

Food Chemistry: X

journal homepage: www.sciencedirect.com/journal/food-chemistry-x

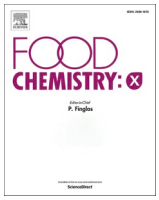

Miniaturized thermal purge-and-trap device combined with self-calibration colorimetric/SERS dual-model optical sensors for highly rapid and selective detection of sulfur dioxide in wine

Yun Wu [a,*], Meiqi Wang [a], Ying Gu [b], Kun Ge [b,*]

[a] College of Food Science and Pharmacy, Xinjiang Agricultural University, Urumqi 830052, China
[b] Faculty of Food Science and Engineering, Kunming University of Science and Technology, Kunming 650500, China

ARTICLE INFO

Keywords:
Miniaturized thermal purge-and-trap (MTPT)
Dual-model optical sensors
Colorimetric
Surface-enhanced Raman spectroscopy
Self-calibration
Sulfur dioxide

ABSTRACT

Herein, the miniaturized thermal purge-and-trap (MTPT) device combined with self-calibration colorimetric/surface-enhanced Raman spectroscopy (SERS) dual-model optical sensors were designed for effective analysis of sulfur dioxide (SO_2) in wine. The SO_2 can be rapidly separated from wine and enriched by MTPT device, ensuring colorimetric/SERS dual-model optical sensing based on Karl Fischer reaction. The high separation efficiency of miniaturized MTPT device combined with self-calibration of dual-model optical sensors significantly alleviate matrix interference and improve the detection accuracy. The satisfactory linear range of 0.1–200.0 mg/L and 0.1–500.0 mg/L with limit of detection of 0.03 mg/L can be obtained. Finally, the MTPT-colorimetric/SERS method was applied to determine the content of SO_2 in different kinds of wine to verify the practicality. These results provide an ideal strategy in construction of MTPT device combined with self-calibration dual-model optical sensors for quantification of gaseous hazards in complex food samples with high rapidity, anti-interference and accuracy.

1. Introduction

Sulfur dioxide (SO_2) is a widely used additive (preservative) in food and drug industries based on the promising antioxidant and antimicrobial performance, preventing the oxidation, microbial spoilage, and color changes induced by enzymatic and non-enzymatic reactions (Gimenez-Gomez et al., 2017; Mu et al., 2022). The advantages of simple operation and low cost made sulfur fumigation very popular in ancient China, especially in storage of Traditional Chinese Medicine (Fan et al., 2022). However, the potential health risk can be caused by SO_2 intake with high concentration, such as asthma attacks, pulmonary edema, and heart disease (Deng et al., 2014; Si et al., 2020). In addition, some diseases including irritation of respiratory and digestive tracts, pulmonary atherosclerosis, and hypertension can be induced by the abnormal fluctuations of endogenous SO_2 concentration levels (Mi et al., 2023). Thus, the monitoring and controlling of potential SO_2 residues in food and drugs is an unavoidable and important task in field of food safety. The maximum allowable level of SO_2 in red and white wines are set to be 160 mg/L and 210 mg/L by European Union legislation, and the obvious reminder of label must be given on the external packing when the total SO_2 content exceeds 10 mg/L (Yan et al., 2022; Zhong et al., 2012). Currently, various analytical methods including chromatography (Koch et al., 2010; Mu et al., 2022), electrochemical method (Doblinger, Lee, Gurnah, & Silvester, 2020; Tian, Qu, & Zeng, 2017), fluorescence method (Ma, Huo, Chao, Li, & Yin, 2020) and colorimetric (Yuan et al., 2023) have been used in the determination of SO_2. Unfortunately, the simplifying of complex sample pre-treatment process in real samples and enhancement of detection accuracy for SO_2 determination is still challengeable.

Generally, the reduce of matrix interference in analysis of real samples still need effective sample pre-treatment methods, mainly including separation and enrichment process for analytes (Jiang, Yang, Tian, & Sun, 2023; Nadar, Patil, & Rohra, 2020; Tapia-Hernández et al., 2019). Various sample pre-treatment methods have been adopted to separate and enrich target molecules for high analysis, such as solid phase micro extraction (SPME) (Yang et al., 2023), headspace micro-extraction (Zhu et al., 2024), liquid−liquid extraction (Marsousi, Karimi-Sabet, Moosavian, & Amini, 2019; Polyakova, Mazur, Artaev, & Lebedev, 2015), magnetic extraction (Mhd Haniffa et al., 2021; Ranc et al., 2014), etc. The above sample pre-treatment methods mainly rely

* Corresponding authors.
E-mail addresses: wuyunster@sina.com (Y. Wu), Gekun@kust.edu.cn (K. Ge).

https://doi.org/10.1016/j.fochx.2024.102091
Received 14 November 2024; Received in revised form 19 November 2024; Accepted 11 December 2024
Available online 12 December 2024

on solid−liquid or liquid−liquid separation-enrichment process, which usually meet limitations in requirement of large amounts of sample solutions and extraction solvent, as well as complex operation and long proceeding time (Z. Chen, Li, & Zhang, 2017). Recently, some sample pre-treatment techniques including SPME and purge-and-trap (P&T) based on solid−gas and liquid−gas separation-enrichment process show superiorities in small amounts of sample solutions and extraction solvent, rapidity, and ignorable cleanup post-treatment (Feng, Yang, Qi, & Li, 2016; Leszczynska, Hallmann, Treder, Baczek, & Roszkowska, 2024; Wieczorek, Zhou, Jelen, & Pawliszyn, 2024). However, the traditional SPME and P&T techniques usually coupling with chromatography including liquid chromatography (−mass spectra) (LC/LC-MS) or gas chromatography (−mass spectra) (GC/GC–MS), meeting limitations in complex operations and slow analysis (da Silva, Vargas Medina, & Lancas, 2021; Fredes et al., 2016). Hence, the development of analytical methods by rapid detection techniques combined with SPME and P&T techniques is a potential ideal strategy for highly rapid and selective analysis of analytes in complex samples.

Currently, the optical sensors including colorimetric, fluorescence, and SERS have been regarded as promising tools for rapid analysis based on their rapidity, convenience, and sensitivity (Kumar, Leray, & Depauw, 2016; L. Zhang, Chen, Wen, Liang, & Qiu, 2019). However, the detection accuracy of general optical sensors still needs to be improved owing to their low stability and repeatability (Ge et al., 2019; Ge, Hu, Zheng, Jiang, & Li, 2021). Thus, many efforts have been tried to improve analysis accuracy of optical sensors. Among various strategies, self-calibration strategy has been widely adopted for detection accuracy improvement thanks to it's convenience and efficient practicality (Chen et al., 2022; Yin et al., 2024). In general, the self-calibration strategy can be realized through internal standard (IS) molecule or multi-modal sensing, providing the effective references for detection accuracy enhancement (Cao et al., 2025). For instance, Chen et al. (Chen et al., 2022) prepared 4-mercaptobenzonitrile (MPBN, internal standard) embedded core-molecule-shell Au nanoflower (Au@MPBN@Au), followed by modification of 4-aminothiophenol (4-ATP, recognition molecule) to obtain Au@MPBN@Au@4-NTP for SERS analysis of H_2S. The Raman peak at 2223 cm^{-1} derived from MPBN was set as IS peak, and peak at 1139 cm^{-1} will be appeared after addition of H_2S. The concentration of H_2S can be accurately labelled based on the ratio of I_{1139}/I_{2223}, improving detection accuracy compared to quantification by single 1139 cm^{-1} peak intensities. In addition, a novel thymine-modified Au nanoparticles/reduced-state sulfur nanodots (T-AuNPs/r-SDs) optical sensor was designed and fabricated by Zhang et al. (Zhang, Li, & Gan, 2023) for colorimetric/fluorescence dual-model detection of Hg^{2+}, exhibiting good analysis accuracy through mutual calibration of dual-model method. Thus, the analytical method based on multi-modal optical sensors coupling with miniaturized P&T device is a promising strategy for highly rapid, selective, and accurate detection of hazards in complex food samples.

In this work, we proposed a novel MTPT device coupling with self-calibration colorimetric/SERS dual-model optical sensors for highly rapid and accurate analysis of SO_2 in wine. The thermal-assisted MTPT device can significantly enhance the detection accuracy by alleviating matrix interference based on high efficiency in separation and enrichment of SO_2 from complex wine sample. Additionally, the dual-model colorimetric/SERS method not only provide specific recognition of SO_2 based on the Karl Fischer reaction, but also improve analytical accuracy via self-calibration function within dual-model optical sensors. The as-developed colorimetric/SERS dual-model method based on MTPT device integrated superiorities of high rapidity, sensitivity and anti-interference in SERS analysis. Finally, the MTPT-colorimetric/SERS method was used for detection of SO_2 in wine samples with good analytical performance. The promising accuracy can be verified through commercial ELISA kit and self-calibration between colorimetric and SERS model. These results proposed an attractive strategy in design and fabrication of MTPT device coupling with dual-model optical sensors with self-calibration function for quantitative analysis of gaseous hazards in complex food samples with high rapidity, anti-interference, and accuracy.

2. Experimental section

2.1. Chemicals and regents

Sodium sulphite (Na_2SO_3, 98 %), starch (99 %), iodine elemental (I_2, 99 %) and potassium iodide (KI, 99 %) were obtained from Shanghai Macklin Biochemical Technology Co., Ltd. (Shanghai, China). 4-Mercaptopyridine (Mpy, 99 %) was purchased from Aladdin Chemistry Co., Ltd. (Shanghai, China). Anhydrous methanol and concentrated sulfuric acid (H_2SO_4, 98 %) were obtained from Sinopharm Chemical Reagent Co., Ltd. (Tianjin, China). Tetrachloroaurate trihydrate ($HAuCl_4{\cdot}3H_2O$, 99.9 %) was provided Shanghai Bide Pharmatech Co., Ltd. (Shanghai, China). The ELISA kit for SO_2 was purchased from Shanghai NEOGEN Biochemical Technology Co., Ltd. (Shanghai, China).

The SO_2 standard solution was prepared by mixing Na_2SO_3 stock solution with different concentrations (0.1–500.0 mg/L, 10.0 mL) and H_2SO_4 stock solution (0.2 mol/L, 1.0 mL). It should be noted that all the stock solution of Na_2SO_3 need to be freshly prepared prior to the use. The colorimetric/SERS dual-model reaction regent was prepared by mixing starch stock solution (0.5 %, *m/v*, 10.0 mL), iodine stock solution (0.2 mL), methanol (10 %, *v/v*, 9.9 mL) and Mpy methanol solution (5.0 mmol/L, 0.1 mL). The iodine stock solution was prepared by dissolving iodine elemental (32.5 mg) and KI (87.5 mg) powder in 10.0 mL pure water. The Milli-Q system was used to product ultrapure deionized purified for all experiments and aqua regia (HCl: HNO_3 = 3:1, *v/v*) was used to clean all of glassware before used.

2.2. Instruments

The UV–Vis and SERS analysis was monitored by Shimadzu UV-2600i spectrophotometer (Shimadzu, Japan) and BWTek BWS465-785S portable Raman spectrometer (λ_{ex} = 785 nm, i-Raman Plus, USA), respectively. The morphology and size distribution of AuNPs was characterized by JEM-F200 transmission electron microscope (TEM, JEOL, Japan) and Malvern Zetasizer Nano ZS90 (Malvern Instruments Ltd., UK), respectively.

2.3. Development of MTPT device

The MTPT system was mainly composed by five parts: a miniaturized carrier gas pump, a flowmeter, a vapor flask, a miniaturized heating device (composed adapter, thermostat and heating jacket), and an adoptor. The miniaturized carrier gas pump was used to carry air gas through whole MTPT system with controllable flow velocity of 0.1–5.0 L/min. The flowmeter with flow speed range of 0.1–5.0 L/min was used to precisely control the flow velocity of miniaturized carrier gas pump. The vapor flask with capacity of 100 mL was placed in heating jacket for holding standard solutions or wine samples. The miniaturized heating device was consisted of a composed adapter, thermostat (with controllable temperature in range of 25–180 °C), and heating jacket for supplying power, controlling temperature, and heating vapor flask, respectively. The heating jacket was customized by heat-resistant fiberglass with similar shapes for vapor flask, ensuring that the vapor flask is tightly wrapped. Finally, the adoptor with capacity of 50 mL was holding colorimetric/SERS dual-model reaction regent for SO_2, consisting of mixture of starch/iodine/Mpy.

2.4. FDTD and DFT simulations

The finite difference time domain (FDTD) method based on COMSOL Multiphysics 5.5 software was used to investigate the electromagnetic field distribution of AuNPs. In Detail, 785 nm incident light irradiated

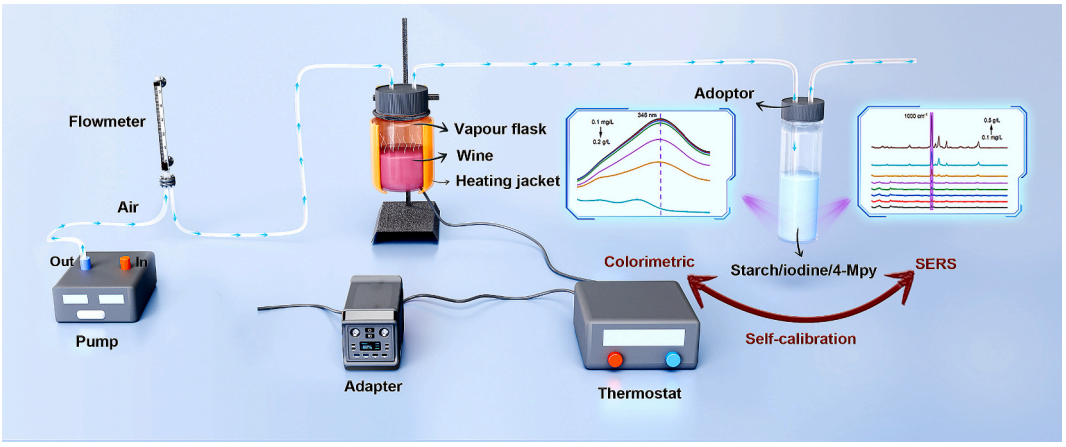

Scheme 1. Schematic illustration of fabrication of MTPT device for self-calibration colorimetric/SERS dual-model optical analysis of SO_2 in wine.

along x-axis and perpendicular to AuNPs in the z-axis. The diameter of AuNPs were set as 40 nm (provided by TEM images) and the Lorentz-Drude was used as dielectric constants of AuNPs. The outmost sides of model diameter of 1.0 μm was confirmed with perfectly matched layer (PML) and the minimum mesh were set to 1.0 nm.

The density functional theory (DFT) was adopted for calculating Gibbs free energy of Karl Fischer reaction by Gaussian 09 software. The optimization of geometric structure and calculation of binding energy was performed by B3LYP method with 6-311G+ (d, p) basis set for most of molecules and I element was calculated by LanL2DZ basis set.

2.5. Dual-model analysis of SO_2 by MTPT device

The MTPT device combined with self-calibration colorimetric/SERS dual-model optical sensors were applied to detection of SO_2 in standard solution and wine samples to validate the feasibility. Typically, 10.0 mL Na_2SO_3 stock solution with concentration in range of 0.1–500.0 mg/L and 1.0 mL H_2SO_4 stock solution (0.2 mol/L) were added into 100 mL vapor flask. For Karl Fischer reaction, 10.0 mL starch stock solution (0.5 %, *m/v*), 0.2 mL iodine stock solution (dissolving 32.5 mg iodine elemental and 87.5 mg KI powder in 10.0 mL pure water), 9.9 mL methanol (10 %, *v/v*), and 0.1 mL Mpy methanol solution (5.0 mmol/L) were added into 50 mL adoptor. After that, connecting different MTPT parts with silicon tube, followed by adjustment of flow velocity (miniaturized carrier gas pump and flowmeter) and temperature (thermostat) with 0.6 L/min and 50 °C, respectively. After thermal purge-and-trap for 6 min, the reaction regent in adoptor was taken out for colorimetric and SERS analysis. For colorimetric analysis, 1.0 mL reaction regent was used for monitoring UV–Vis absorbance. For SERS analysis, 0.16 mL reaction regent was mixed with 0.16 mL AuNPs in 96-pore plate for monitoring Raman spectrum. Three wine samples were collected from local supermarket for determining the content of SO_2. The Na_2SO_3 stock solution (10.0 mL) was replaced by wine sample (10.0 mL) in vapor flask, and other process was similar with SO_2 standard solution mentioned above. The UV–Vis parameters are listed as follows: wavelength range: 200–400 nm; scanning speed: low; scanning slit: 2 nm. The SERS parameters are listed as follows: excitation wavelength: 785 nm; wavelength range: 200–2000 cm^{-1}; laser power: 105 mW; integral time: 5 s. The parallel three samples were measured and each UV–Vis and SERS measurement was repeated three times.

3. Results and discussion

3.1. Design of MTPT device

The MTPT device coupling with colorimetric/SERS dual-model optical sensors for highly effective analysis of SO_2 in wine was illustrated in

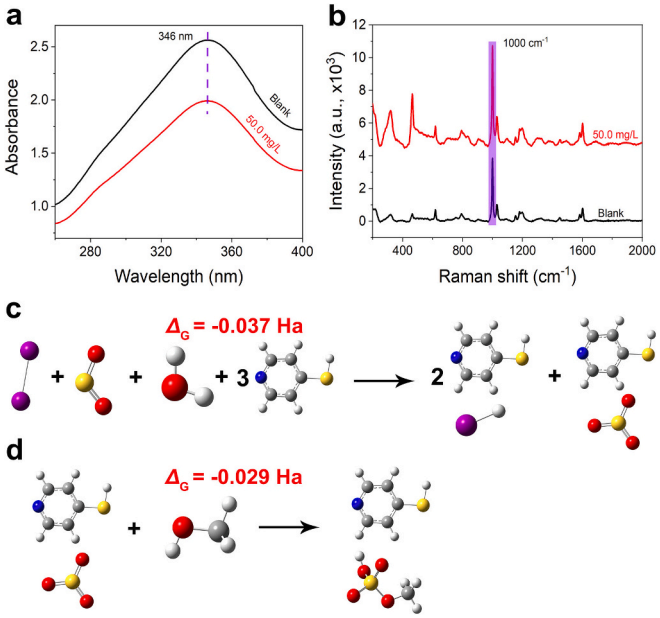

Fig. 1. The feasibility of colorimetric (a) and SERS (b) analysis of SO_2 by Karl Fischer reaction. (c–d) Schematic diagram of the reaction process of Karl Fischer reaction.

Scheme 1. The digital photograph can be seen in Fig. S1 in Supplementary Material. The high efficiency of separation and enrichment for SO_2 from complex wine sample by MTPT device and improved accuracy induced by self-calibration of dual-model optical methods ensuring the satisfied analytical performance within 6 min. On the one hand, the thermal-assisted MTPT device can alleviate matrix interference via effective liquid−gas extraction-separation process. On the other hand, the dual-model colorimetric/SERS optical sensors based on the Karl Fischer reaction will ensure the specific recognition of SO_2, as well as enhancing analytical accuracy through self-calibration function between colorimetric and SERS method. The Karl Fischer reaction results in discoloration of starch-iodine mixture, and the formation of pyridine methyl sulfate will be further for formed in the presence of Mpy and methanol. The overall two-step reaction process can be seen as follows (Li, Duan, Ma, & Deng, 2018),

$$I_2 + SO_2 + H_2O + 3Mpy \rightarrow 2Mpy{\cdot}HI + Mpy{\cdot}SO_3 \quad (1)$$

$$Mpy{\cdot}SO_3 + CH_3OH \rightarrow Mpy{\cdot}HSO_4CH_3 \quad (2)$$

After Karl Fischer reaction process, the absorbance and SERS

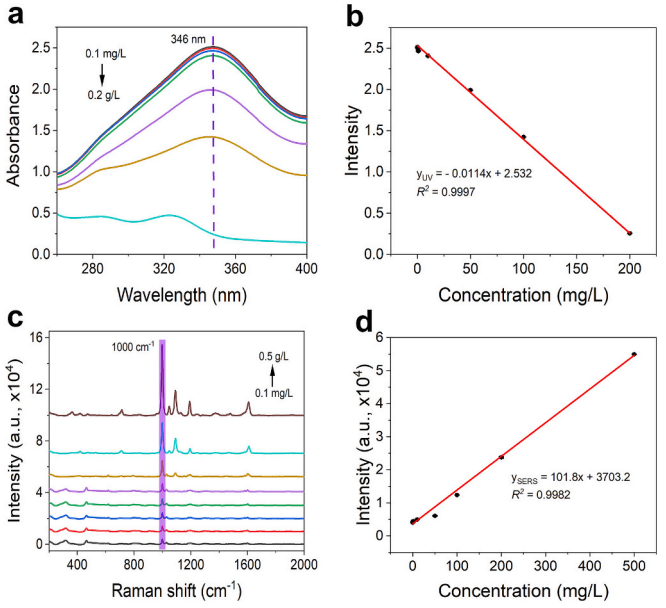

Fig. 2. The UV–Vis (a) and SERS (c) intensity of SO_2 at different concentration. Plot of UV–Vis (b) and SERS (d) against SO_2 concentration with the linear range from 0.1 to 200.0 mg/L and 0.1 to 500.0 mg/L, respectively.

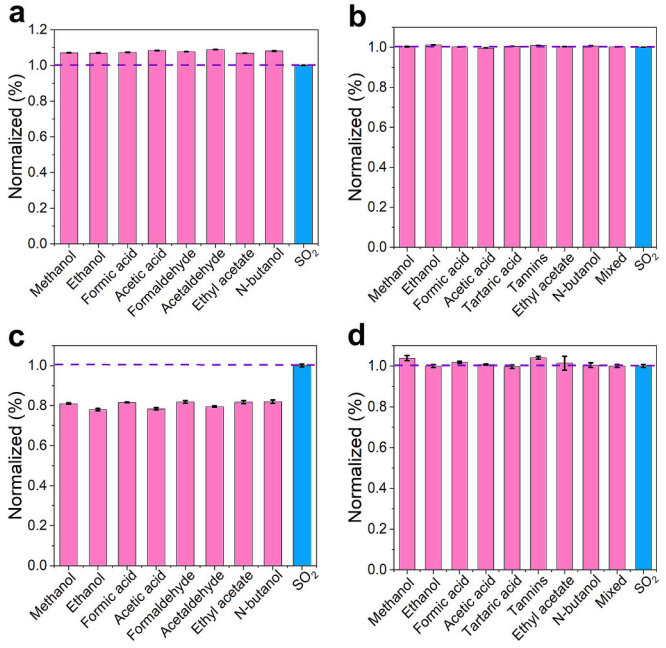

Fig. 3. Selectivity of MTPT device for 10.0 mg/L SO_2 over other interfering substance by colorimetric (a) and SERS (c) method (100-folds). Anti-interference ability of MTPT device for 10.0 mg/L SO_2 over other interfering substance by colorimetric (b) and SERS (d) method (100-folds).

intensity of reaction mixture will be decreased and increased, respectively. Thus, the concentrations of SO_2 can be confirmed according to the absorbance and SERS intensity.

3.2. The feasibility of MTPT-colorimetric/SERS strategy

On the basis of the high efficiency of separation and enrichment for SO_2 by self-made MTPT device, we propose a colorimetric/SERS dual-model method for highly accurate analysis of SO_2 based on typical Karl Fischer reaction between SO_2 and starch/iodine/Mpy mixture. As shown in Fig. 1a, the blank sample displayed high UV–Vis absorbance of 2.56 at 246 nm, while the absorbance descended to 1.99 in the presence of 50.0 mg/L Na_2SO_3. The Raman intensity at 1000 cm^{-1} was significantly increased from 3862.1 a.u. to 6072.4 a.u. after addition of 50.0 mg/L Na_2SO_3 (Fig. 1b). The above results suggest the feasibility of MTPT-colorimetric/SERS strategy for high analysis of SO_2. In addition, the two-step Karl Fischer reaction process was further calculated by density functional theory (DFT) with Gibbs free energy (Δ_G). As it can be seen in Fig. 1c, d, the Δ_G for reaction (1) and (2) was −0.037 and − 0.029 Ha, indicating the feasibility of Karl Fischer reaction between SO_2 and starch/iodine/Mpy mixture, further confirming the feasibility of MTPT-colorimetric/SERS strategy for high analysis of SO_2. The characterizations of AuNPs including TEM, UV–Vis absorption spectra, and dynamic light scattering (DLS) analysis were provided in Fig. S2, proving the successful preparation of AuNPs for SERS model. Furthermore, the possible electromagnetic field distribution of AuNPs was investigated by FDTD simulations (Fig. S3). The AuNPs display strong electromagnetic field strength in the vicinity of AuNPs, suggesting the high Raman enhancement for analysis of SO_2 based on SERS model.

3.3. Optimization of MTPT-colorimetric/SERS dual-model method

The analytical performance of MTPT-colorimetric/SERS method is affected by several parameters. Thus, reaction time, heating temperature, and velocity of flow show obvious impact for colorimetric/SERS dual-model analysis of SO_2. The reaction time is important for separation and enrichment of SO_2 from liquid sample, as well as Karl Fischer reaction between SO_2 and starch/iodine/Mpy mixture. Fig. S4a, d shows that the UV–Vis absorbance (346 nm) and Raman intensity (1000 cm^{-1}) decreases and increases significantly as the reaction time in the range of 1–6 min in the presence of 50.0 mg/L Na_2SO_3. After 6 min, the UV–Vis absorbance and Raman intensity show opposite trend. Additionally, heating temperature can affect the separation and enrichment efficiency of SO_2, thus show significance to strengthen sensitivity for analysis of SO_2 based on colorimetric/SERS dual-model method. As shown in Fig. S4b, e, MTPT-colorimetric/SERS method treated with different heating temperature (30–70 °C) yielded different UV–Vis absorbance and Raman intensity at 346 nm and 1000 cm^{-1}, respectively. The UV–Vis absorbance and Raman intensity decreased and increased as the heating temperature increased from 30 to 50 °C, and then shows upward and downward trend, respectively. Finally, the velocity of flow is of significance to ensure separation, enrichment efficiency and Karl Fischer reaction. As it can be seen in Fig. S4c, f, the lowest UV–Vis absorbance (346 nm) and highest Raman intensity (1000 cm^{-1}) can be reached while the velocity of flow is 0.6 mL/min in the presence of 50.0 mg/L Na_2SO_3. Hence, 6 min of reaction time, 50 °C of heating temperature, and 0.6 mL/min of velocity of flow were used for colorimetric/SERS dual-model analysis of SO_2.

3.4. Development of colorimetric/SERS dual-model method for analysis of SO_2

Under the optimum experimental parameters, the linear relationship between the concentrations of SO_2 and the spectral intensity (UV–Vis and SERS model) were investigated (Fig. 2). As shown in Fig. 2a, c, the UV–Vis absorbance at 346 nm and SERS intensity at 1000 cm^{-1} were obviously decreased and increased with the increase of concentration of Na_2SO_3, and the corresponding photographs can be seen in Fig. S5. The linear relationship between concentrations of Na_2SO_3 and the spectral intensity were established with correlation coefficient (R^2) of 0.9997 and 0.9982 for UV–Vis (0.1 mg/L–0.2 g/L) and SERS (0.1 mg/L–0.5 g/L) model, respectively (Fig. 2b, d). The LOD for SO_2 with UV–Vis and SERS model can be obtained with 0.03 mg/L based on rules of $3\sigma/k$. The superiorities of as-developed MTPT-colorimetric/SERS method can be found in rapidity, sensitivity, and self-calibration compared to previous reported methods (Table S1).

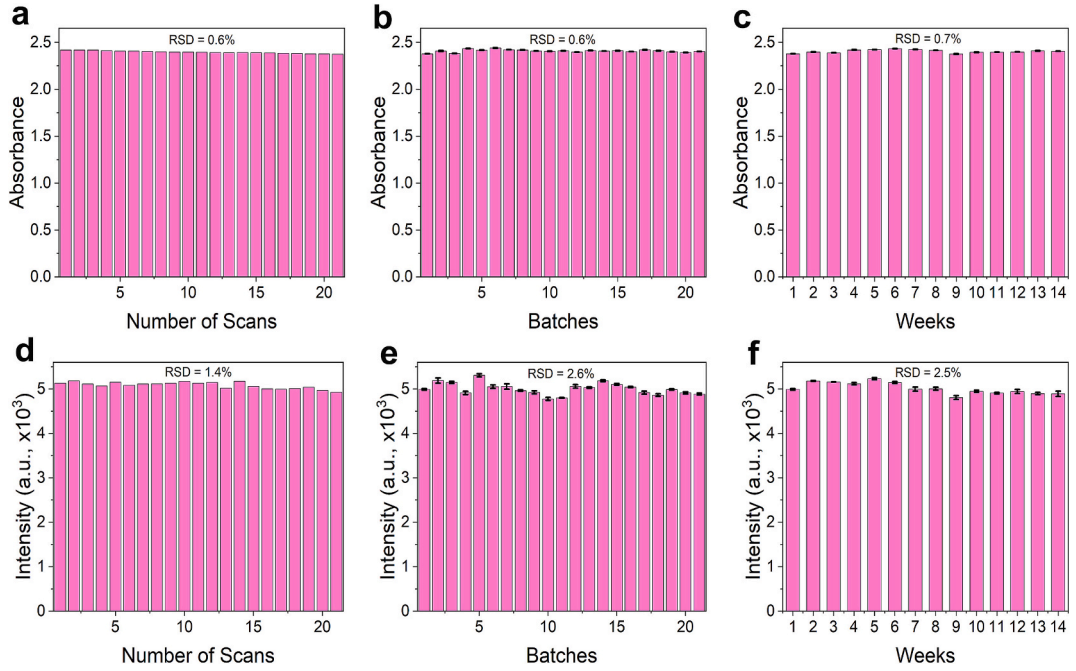

Fig. 4. Stability of MTPT device for detecting 10.0 mg/L of SO_2 in 21 replicates (a, d), 21 different batches (b, e), 14 consecutive weeks (c, f) by colorimetric (a–c) and SERS (d–f) method.

The investigation of selectivity and anti-interference ability for as-developed MTPT-colorimetric/SERS method was essential for complex sample analysis. As displayed in Fig. 3a, c, several analogues (methanol, ethanol, formic acid, acetic acid, formaldehyde, acetaldehyde, ethyl acetate, and N-butanol, 100-folds) for SO_2 exhibit negligible effect on UV–Vis absorbance at 346 nm and SERS quantitative peak at 1000 cm^{-1} compared to Na_2SO_3 with 10.0 mg/L. Furthermore, the anti-interference ability of MTPT-colorimetric/SERS method for potential interferences (methanol, ethanol, formic acid, acetic acid, tartaric acid, tannins, ethyl acetate, N-butanol, and mixed) was further evaluated before the practical analysis of SO_2 in wine. As shown in Fig. 3b, d, the above interfering substances not affect UV–Vis absorbance at 346 nm and SERS quantitative peak at 1000 cm^{-1} in the presence of Na_2SO_3 (10.0 mg/L). The above selectivity and anti-interference results suggest the high feasibility in rapid and accurate analysis of SO_2 in real wine sample by as-developed MTPT-colorimetric/SERS method.

3.5. Stability and repeatability

Furthermore, the as-developed MTPT-colorimetric/SERS method for high analysis of SO_2 was investigated in stability and repeatability. Firstly, the measurements by colorimetric and SERS model for 11

Table 1
Analysis of SO_2 in wine samples with MTPT-colorimetric/SERS and ELISA method.

Sample	UV–Vis method		SERS method		Kit method		Difference between UV–Vis and SERS (%)	Difference between UV–Vis and Kit (%)	Difference between SERS and Kit (%)
	determined (mg/kg)	RSD (%, *n* = 3)	determined (mg/kg)	RSD (%, *n* = 3)	determined (mg/kg)	RSD (%, n = 3)			
Dry red wine 1	N.D.[a]	/	N.D.	/	N.D.	/	/	/	/
Dry red wine 2	N.D.	/	N.D.	/	N.D.	/	/	/	/
Sweat red wine 1	N.D.	/	N.D.	/	N.D.	/	/	/	/
Sweat red wine 2	N.D.	/	N.D.	/	N.D.	/	/	/	/
Dry white wine 1	450.4	0.2	435.7	1.0	432.3	0.2	3.4	4.2	0.8
Dry white wine 2	195.7	0.7	186.8	0.4	197.3	0.2	4.8	−0.8	−5.3
Sweat white wine 1	146.6	0.2	142.2	0.7	144.1	0.3	3.1	1.7	−1.3
Sweat white wine 1	187.6	0.5	182.0	0.3	186.6	0.3	3.1	0.5	−2.5
Meijiu 1	34.5	0.1	32.6	0.4	32.8	0.1	5.8	5.2	−0.6
Meijiu 2	N.D.	/	N.D.	/	N.D.	/	/	/	/

Difference (%) = $[C_{(SERS\ method)} - C_{(Kit\ method)}]/C_{(Kit\ method)} \times 100$ %.
Difference (%) = $[C_{(UV–Vis\ method)} - C_{(Kit\ method)}]/C_{(Kit\ method)} \times 100$ %.
Difference (%) = $[C_{(UV–Vis\ method)} - C_{(SERS\ method)}]/C_{(UV–Vis\ method)} \times 100$ %.
[a] N.D. = Not detected.

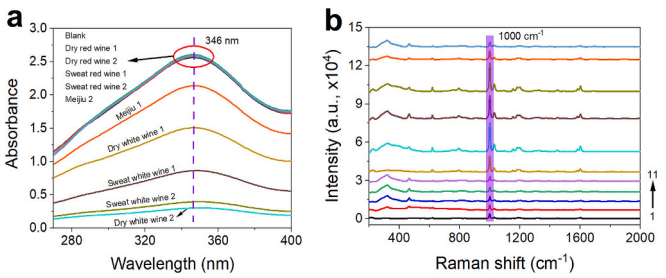

Fig. 5. UV–Vis absorption (a) and SERS (b, line 1–11) spectra of blank, dry red wine 1, dry red wine 2, sweat red wine 1, sweat red wine 2, dry white wine 1, dry white wine 2, sweat white wine 1, sweat white wine 2, Meijiu 1, and Meijiu 2 samples. (For interpretation of the references to color in this figure legend, the reader is referred to the web version of this article.)

replicate scans of 10.0 mg/L Na_2SO_3 can be sen in Fig. 4a, d with low RSDs of 0.6 % and 1.4 %, respectively. In addition, the RSDs for 21 batches of starch/iodine/Mpy mixture with addition of 10.0 mg/L Na_2SO_3 were 0.6 % and 2.6 % for colorimetric and SERS model, respectively (Fig. 4b, e). Finally, the interday detection precision of starch/iodine/Mpy mixture were evaluated in 14 consecutive weeks with RSDs of 0.7 % and 2.5 % in the presence of 10.0 mg/L Na_2SO_3 for colorimetric and SERS model, respectively (Fig. 4c, f). The high feasibility of colorimetric/SERS dual model for SO_2 detection in several conditions can be guaranteed based on the satisfied repeatability and reproducibility of developed MTPT-colorimetric/SERS method.

3.6. Analytical applications in wine samples

In the next, the as-developed MTPT-colorimetric/SERS method was applied to quantitative detection of SO_2 in 5 kinds of wine sample including dry red wine, sweat red wine, dry white wine, sweat white wine, and Meijiu. As displayed in Table 1, the concentration of 450.4, 195.7, 146.6, 187.6, 34.5 mg/kg (colorimetric model) and 435.7, 186.8, 142.2, 182.0, 32.6 mg/kg (SERS model) in dry white wine 1, dry white wine 2, sweat white wine 1, sweat white wine 2, and Meijiu 1, respectively; and no SO_2 was found in dry red wine, sweat red wine, and Meijiu 2 sample. The corresponding UV–Vis absorption and SERS spectra of wine samples can be seen in Fig. 5. The relative errors between colorimetric and SERS model are in range of 3.1–5.8 %, indicating great self-calibration function for accurate analysis of SO_2 in wine (Table 1). It could be concluded that SO_2 are more likely to be used in white wine due to the purpose of bleaching, which is consistent with previously reported results (Cho, JaeJeon, GyungyunChung, & YongsungLee, 2021; Li et al., 2018). Comparing to previous reported methods, the as-developed MTPT-colorimetric/SERS method show comprehensive advantages in rapidity, sensitivity, and self-calibration (Table S1). In addition, the ELISA method (Fig. S6) was also adopted to validate the accuracy of the colorimetric/SERS dual-model method. The relative errors between ELISA method and colorimetric/SERS dual-model method are ranging from −5.3 % to 5.2 % (Table 1). Additionally, Table 2 displays the recoveries of three wine samples ranging from 89.1 to 114.7 % with low detection RSDs of 0.1–1.8 %, indicating the high accuracy of proposed MTPT-colorimetric/SERS method. The above analytical application results indicate that the proposed method shows high reliability and accuracy in rapid, accurate, and quantitative analysis of SO_2 in wine samples.

4. Conclusions

In summary, a novel MTPT device coupling with self-calibration colorimetric/SERS dual-model optical sensors was developed for rapid, accurate and quantitative detection of SO_2 in wine. The thermal-assisted MTPT device show high efficiency in separation and enrichment

Table 2
Recovery analysis of SO_2 in wine samples with MTPT-colorimetric/SERS method.

Sample	Kit method (mg/kg)	Assay	Added (mg/kg)	Found (mg/kg)	Recovery (%)	RSD (%, n = 3)
Dry red wine 1	N.D.[a]	UV–Vis method	1.0	1.1	105.2	0.1
			10.0	10.0	99.7	0.1
			100.0	105.5	105.5	0.1
		SERS method	1.0	1.0	99.7	0.5
			10.0	10.4	103.8	1.8
			100.0	100.2	100.2	1.6
Dry red wine 2	N.D.	UV–Vis method	1.0	1.1	108.7	0.1
			10.0	11.2	112.0	0.2
			100.0	96.9	96.9	0.1
		SERS method	1.0	1.1	114.3	1.0
			10.0	9.2	92.2	0.5
			100.0	92.0	92.0	0.2
Sweat red wine 1	N.D.	UV–Vis method	1.0	1.1	111.5	0.1
			10.0	10.3	103.3	0.1
			100.0	97.3	97.3	0.1
		SERS method	1.0	1.1	111.8	0.5
			10.0	9.9	99.4	1.0
			100.0	107.3	107.3	0.4
Sweat red wine 2	N.D.	UV–Vis method	1.0	1.0	102.6	0.1
			10.0	10.8	108.3	0.1
			100.0	103.0	103.0	0.1
		SERS method	1.0	1.0	98.6	0.1
			10.0	9.8	98.0	0.4
			100.0	103.4	103.4	0.6
Dry white wine 1	432.3	UV–Vis method	1.0	437.8	101.0	0.2
			10.0	421.4	95.3	0.1
			100.0	532.1	100.0	0.1
		SERS method	1.0	409.1	94.4	0.1
			10.0	466.1	105.4	0.4
			100.0	522.1	98.1	0.3
Dry white wine 2	197.3	UV–Vis method	1.0	211.0	106.4	0.1
			10.0	191.7	92.5	0.1
			100.0	271.5	91.3	0.1
		SERS method	1.0	176.7	89.1	0.5
			10.0	206.3	99.5	0.2
			100.0	325.8	109.6	0.3
Sweat white wine 1	144.1	UV–Vis method	1.0	133.0	91.6	0.1
			10.0	163.2	105.9	0.1
			100.0	245.4	100.5	0.3
		SERS method	1.0	150.1	103.4	0.1
			10.0	172.3	111.8	0.3
			100.0	240.4	98.5	1.1
Sweat white wine 2	186.6	UV–Vis method	1.0	192.2	102.4	0.1
			10.0	192.4	97.9	0.1
			100.0	263.1	91.8	0.1
		SERS method	1.0	198.4	105.7	0.3
			10.0	220.5	112.1	0.2
			100.0	282.5	98.6	1.0
Meijiu 1	32.8	UV–Vis method	1.0	32.6	91.3	0.1
			10.0	43.6	101.8	0.1
			100.0	120.5	90.7	0.5
		SERS method	1.0	34.1	100.9	0.7
			10.0	40.9	95.6	0.2
			100.0	141.2	106.3	0.6
Meijiu 2	N.D.	UV–Vis method	1.0	1.1	105.1	0.1
			10.0	11.5	114.7	0.1
			100.0	107.0	107.0	0.1

(continued on next page)

Table 2 (*continued*)

Sample	Kit method (mg/kg)	Assay	Added (mg/kg)	Found (mg/kg)	Recovery (%)	RSD (%, n = 3)
		SERS method	1.0	1.0	99.6	0.4
			10.0	9.8	98.0	0.9
			100.0	92.3	92.3	0.1

[a] N.D. = Not detected.

of SO_2 from complex wine sample, enhancing the detection accuracy by alleviating matrix interference. In addition, the dual-model colorimetric/SERS optical sensors not only provide specific recognition of SO_2 based on the Karl Fischer reaction, but also improve analytical accuracy via self-calibration function between colorimetric and SERS model. The high selectivity and anti-interference ability of MTPT-colorimetric/SERS method can be obtained. In addition, high stability and repeatability guarantee the feasibility in SO_2 detection by colorimetric/SERS dual model in several conditions. Finally, the MTPT-colorimetric/SERS method was applied to quantitative analysis of SO_2 in real wine samples, showing great analytical performance including linear range, LOD, accuracy and recovery. These results provide a new strategy in design and fabrication of MTPT device coupling with self-calibration dual-model optical sensors for quantification of gaseous hazards in complex food samples with high rapidity, anti-interference, and accuracy.

CRediT authorship contribution statement

Yun Wu: Writing – review & editing, Writing – original draft, Supervision, Conceptualization. **Meiqi Wang:** Formal analysis, Data curation. **Ying Gu:** Formal analysis, Data curation. **Kun Ge:** Writing – review & editing, Supervision, Conceptualization.

Declaration of competing interest

The authors declare that they have no known competing financial interests or personal relationships that could have appeared to influence the work reported in this paper.

Acknowledgements

The work was funded by the Xinjiang 14th Five-Year Major Scientific and Technological Special Projects (Grant No. 2022A02002-2), the Xinjiang Wine Industry Innovation Research Institute Project (Grant No. 2024650005000023), and the Xinjiang Major Scientific and Technological Projects (Grant No. 2023B02027).

Appendix A. Supplementary data

Supplementary data to this article can be found online at https://doi.org/10.1016/j.fochx.2024.102091.

Data availability

Data will be made available on request.

References

Cao, L., Ye, Q., Ren, Y., Gao, B., Wu, Y., Zhao, X., … Wu, Q. (2025). Nanomaterial-mediated self-calibrating biosensors for ultra-precise detection of food hazards: Recent advances and new horizons. *Coordination Chemistry Reviews, 522*, Article 216204. https://doi.org/10.1016/j.ccr.2024.216204

Chen, S., Fan, J., Lv, M., Hua, C., Liang, G., & Zhang, S. (2022). Internal standard assisted surface-enhanced Raman scattering Nanoprobe with 4-NTP as recognition unit for Ratiometric imaging hydrogen sulfide in living cells. *Analytical Chemistry, 94*(42), 14675–14681. https://doi.org/10.1021/acs.analchem.2c02961

Chen, X., Huang, Q., Ruan, S., Luo, F., You, R., Feng, S., … Lu, Y. (2022). Self-calibration SERS sensor with "core-satellite" structure for detection of hyaluronidase activity. *Analytica Chimica Acta, 1227*, Article 340302. https://doi.org/10.1016/j.aca.2022.340302

Chen, Z., Li, G., & Zhang, Z. (2017). Miniaturized thermal-assisted purge-and-trap technique coupling with surface-enhanced Raman scattering for trace analysis of complex samples. *Analytical Chemistry, 89*(17), 9593–9600. https://doi.org/10.1021/acs.analchem.7b02912

Cho, Y. S., JaeJeon, J., GyungyunChung, M.-S. J., YongsungLee, K.-W., & J Food Control. (2021). Total SO_2 levels and risk assessment of wine and fruit wine consumed in South Korea. *Food Control, 127*(1), Article 108124. https://doi.org/10.1016/j.foodcont.2021.108124

Deng, Z., Chen, X., Wang, Y., Fang, E., Zhang, Z., & Chen, X. (2014). Headspace thin-film microextraction coupled with surface-enhanced Raman scattering as a facile method for reproducible and specific detection of sulfur dioxide in wine. *Analytical Chemistry, 87*(1), 633–640. https://doi.org/10.1021/ac503341g

Doblinger, S., Lee, J., Gurnah, Z., & Silvester, D. S. (2020). Detection of sulfur dioxide at low parts-per-million concentrations using low-cost planar electrodes with ionic liquid electrolytes. *Analytica Chimica Acta, 1124*, 156–165. https://doi.org/10.1016/j.aca.2020.05.037

Fan, B., Wang, Y., Li, Z., Xun, D., Dong, J., Zhao, X., … Wang, Y. (2022). Si@ag@PEI substrate-based SERS sensor for rapid detection of illegally adulterated sulfur dioxide in traditional Chinese medicine. *Talanta, 238*(Pt 1), Article 122988. https://doi.org/10.1016/j.talanta.2021.122988

Feng, D., Yang, H., Qi, D., & Li, Z. (2016). Extraction, confirmation, and screening of non-target compounds in silicone rubber teats by purge-and-trap and SPME combined with GC-MS. *Polymer Testing, 56*, 91–98. https://doi.org/10.1016/j.polymertesting.2016.09.021

Fredes, A., Sales, C., Barreda, M., Valcarcel, M., Rosello, S., & Beltran, J. (2016). Quantification of prominent volatile compounds responsible for muskmelon and watermelon aroma by purge and trap extraction followed by gas chromatography-mass spectrometry determination. *Food Chemistry, 190*, 689–700. https://doi.org/10.1016/j.foodchem.2015.06.011

Ge, K., Hu, Y., Zheng, Y., Jiang, P., & Li, G. (2021). Aptamer/derivatization-based surface-enhanced Raman scattering membrane assembly for selective analysis of melamine and formaldehyde in migration of melamine kitchenware. *Talanta, 235*, Article 122743. https://doi.org/10.1016/j.talanta.2021.122743

Ge, K., Liu, J., Wang, P., Fang, G., Zhang, D., & Wang, S. (2019). Near-infrared-emitting persistent luminescent nanoparticles modified with gold nanorods as multifunctional probes for detection of arsenic(III). *Microchimica Acta, 186*(3), 197. https://doi.org/10.1007/s00604-019-3294-z

Gimenez-Gomez, P., Gutierrez-Capitan, M., Puig-Pujol, A., Capdevila, F., Munoz, S., Tobena, A., … Jimenez-Jorquera, C. (2017). Analysis of free and total sulfur dioxide in wine by using a gas-diffusion analytical system with pH detection. *Food Chemistry, 228*, 518–525. https://doi.org/10.1016/j.foodchem.2017.02.026

Jiang, H., Yang, S., Tian, H., & Sun, B. (2023). Research progress in the use of liquid-liquid extraction for food flavour analysis. *Trends in Food Science & Technology, 132*, 138–149. https://doi.org/10.1016/j.tifs.2023.01.005

Koch, M., Ko?Ppen, R., Siegel, D., Witt, A., Nehls, I. J. J. O. A., & Chemistry, F. (2010). Determination of Total sulfite in wine by ion chromatography after in-sample oxidation. *Journal of Agricultural and Food Chemistry, 58*(17), 9463–9467. https://doi.org/10.1021/jf102086x

Kumar, N., Leray, I., & Depauw, A. (2016). Chemically derived optical sensors for the detection of cesium ions. *Coordination Chemistry Reviews, 310*, 1–15. https://doi.org/10.1016/j.ccr.2015.11.008

Leszczynska, D., Hallmann, A., Treder, N., Baczek, T., & Roszkowska, A. (2024). Recent advances in the use of SPME for drug analysis in clinical, toxicological, and forensic medicine studies. *Talanta, 270*, Article 125613. https://doi.org/10.1016/j.talanta.2023.125613

Li, D., Duan, H., Ma, Y., & Deng, W. (2018). Headspace-sampling paper-based analytical device for colorimetric/surface-enhanced Raman scattering dual sensing of sulfur dioxide in wine. *Analytical Chemistry, 90*(9), 5719–5727. https://doi.org/10.1021/acs.analchem.8b00016

Ma, T., Huo, F., Chao, J., Li, J., & Yin, C. (2020). A highly sensitive ratiometric fluorescent probe for real-time monitoring sulfur dioxide as the viscosity change in living cells and mice. *Sensors and Actuators B: Chemical, 320*, Article 128044. https://doi.org/10.1016/j.snb.2020.128044

Marsousi, S., Karimi-Sabet, J., Moosavian, M. A., & Amini, Y. (2019). Liquid-liquid extraction of calcium using ionic liquids in spiral microfluidics. *Chemical Engineering Journal, 356*, 492–505. https://doi.org/10.1016/j.cej.2018.09.030

Mhd Haniffa, M. A. C., Ching, Y. C., Illias, H. A., Munawar, K., Ibrahim, S., Nguyen, D. H., & Chuah, C. H. (2021). Cellulose supported promising magnetic sorbents for magnetic solid-phase extraction: A review. *Carbohydrate Polymers, 253*, Article 117245. https://doi.org/10.1016/j.carbpol.2020.117245

Mi, W., Shen, T., Guo, X., Liu, X., Zhang, M., & Jia, M. (2023). Ratiometric quantification and visual detection of sulfur dioxide residues using a coumarin-derived fluorescent probe. *Sensors and Actuators B: Chemical, 395*, Article 134459. https://doi.org/10.1016/j.snb.2023.134459

Mu, L., Li, G., Kang, Q., Xu, Y., Fu, Y., & Ye, L. (2022). Determination of sulfur dioxide in food by liquid chromatography with pre-column derivatization. *Food Control, 132*, Article 108500. https://doi.org/10.1016/j.foodcont.2021.108500

Nadar, S. S., Patil, P. D., & Rohra, N. M. (2020). Magnetic nanobiocatalyst for extraction of bioactive ingredients: A novel approach. *Trends in Food Science & Technology, 103*, 225–238. https://doi.org/10.1016/j.tifs.2020.07.007

Polyakova, O. V., Mazur, D. M., Artaev, V. B., & Lebedev, A. T. (2015). Rapid liquid–liquid extraction for the reliable GC/MS analysis of volatile priority pollutants. *Environmental Chemistry Letters, 14*(2), 251–257. https://doi.org/10.1007/s10311-015-0544-0

Ranc, V., Markova, Z., Hajduch, M., Prucek, R., Kvitek, L., Kaslik, J., … Zboril, R. (2014). Magnetically assisted surface-enhanced raman scattering selective determination of dopamine in an artificial cerebrospinal fluid and a mouse striatum using Fe_3O_4/ag nanocomposite. *Analytical Chemistry, 86*(6), 2939–2946. https://doi.org/10.1021/ac500394g

Si, W., Du, W., Wang, F., Wu, L., Liu, J., Liu, W., … Zhang, X. (2020). One-pot hydrothermal synthesis of nano-sheet assembled NiO/ZnO microspheres for efficient sulfur dioxide detection. *Ceramics International, 46*(6), 7279–7287. https://doi.org/10.1016/j.ceramint.2019.11.222

da Silva, L. F., Vargas Medina, D. A., & Lancas, F. M. (2021). Automated needle-sleeve based online hyphenation of solid-phase microextraction and liquid chromatography. *Talanta, 221*, Article 121608. https://doi.org/10.1016/j.talanta.2020.121608

Tapia-Hernández, J. A., Del-Toro-Sánchez, C. L., Cinco-Moroyoqui, F. J., Juárez-Onofre, J. E., Ruiz-Cruz, S., Carvajal-Millan, E., … Rodríguez-Felix, F. (2019). Prolamins from cereal by-products: Classification, extraction, characterization and its applications in micro- and nanofabrication. *Trends in Food Science & Technology, 90*, 111–132. https://doi.org/10.1016/j.tifs.2019.06.005

Tian, Y., Qu, K., & Zeng, X. (2017). Investigation into the ring-substituted polyanilines and their application for the detection and adsorption of sulfur dioxide. *Sensors and Actuators B: Chemical, 249*, 423–430. https://doi.org/10.1016/j.snb.2017.04.057

Wieczorek, M. N., Zhou, W., Jelen, H. H., & Pawliszyn, J. (2024). Automated sequential SPME addressing the displacement effect in food samples. *Food Chemistry, 439*, Article 138093. https://doi.org/10.1016/j.foodchem.2023.138093

Yan, F., Cui, J., Wang, C., Tian, X., Li, D., Wang, Y., … Ma, X. (2022). Real-time quantification for sulfite using a turn-on NIR fluorescent probe equipped with a portable fluorescence detector. *Chinese Chemical Letters, 33*(9), 4219–4222. https://doi.org/10.1016/j.cclet.2022.03.006

Yang, Y., Guo, Y., Jia, X., Zhang, Q., Mao, J., Feng, Y., … Zhang, W. (2023). An ultrastable 2D covalent organic framework coating for headspace solid-phase microextraction of organochlorine pesticides in environmental water. *Journal of Hazardous Materials, 452*, Article 131228. https://doi.org/10.1016/j.jhazmat.2023.131228

Yin, M., Jiao, J., Lu, L., Hu, B., Xue, L., Dai, F., … Chen, Q. (2024). A simultaneous strategy with multiple-signal amplification and self-calibration for ultrasensitive assay of miRNA-21 based on 3D MNPs-IL-rGO-AuNPs. *Biosensors & Bioelectrons, 249*, Article 116009. https://doi.org/10.1016/j.bios.2024.116009

Yuan, L., Gao, M., Xiang, H., Zhou, Z., Yu, D., & Yan, R. (2023). A biomass-based colorimetric sulfur dioxide gas sensor for smart packaging. *ACS Nano, 17*(7), 6849–6856. https://doi.org/10.1021/acsnano.3c00530

Zhang, H., Li, Y., & Gan, F. (2023). Design and fabrication of dual functional sulfur nanodots with reducibility and fluorescence properties for sensitive and selective analysis of metal ions in environmental water samples. *Sensors and Actuators B: Chemical, 374*, Article 132817. https://doi.org/10.1016/j.snb.2022.132817

Zhang, L., Chen, X.-R., Wen, S.-H., Liang, R.-P., & Qiu, J.-D. (2019). Optical sensors for inorganic arsenic detection. *TrAC Trends in Analytical Chemistry, 118*, 869–879. https://doi.org/10.1016/j.trac.2019.07.013

Zhong, Z., Li, G., Zhu, B., Luo, Z., Huang, L., & Wu, X. (2012). A rapid distillation method coupled with ion chromatography for the determination of total Sulphur dioxide in foods. *Food Chemistry, 131*(3), 1044–1050. https://doi.org/10.1016/j.foodchem.2011.09.086

Zhu, S., Lou, X., Zhu, J., Song, Z., Hao, Y., Yang, J., & Lu, M. (2024). Ultra-stable Co_3O_4/$NiCo_2O_4$ double-shelled hollow nanocages as headspace solid-phase microextraction coating for enhanced capture of polychlorinated biphenyls. *Chemical Engineering Journal, 488*, Article 150876. https://doi.org/10.1016/j.cej.2024.150876